Spectrochimica Acta Part A: Molecular and Biomolecular Spectroscopy 137 (2015) 692–700

Contents lists available at ScienceDirect

Spectrochimica Acta Part A: Molecular and Biomolecular Spectroscopy

journal homepage: www.elsevier.com/locate/saa

Structural, spectroscopic and DFT study of 4-methoxybenzohydrazide Schiff bases. A new series of polyfunctional ligands

Verónica Ferraresi-Curotto [a,b], Gustavo A. Echeverría [c], Oscar E. Piro [c], Reinaldo Pis-Diez [a], Ana C. González-Baró [a,*]

[a] CEQUINOR (CONICET, UNLP), CC 962, B1900AVV La Plata, Argentina
[b] Depto. de Química, FACEyN-UNCa, Av. Belgrano 300, K4700AAP Catamarca, Argentina
[c] IFLP (CONICET, UNLP), CC 67, B1900AVV La Plata, Argentina

HIGHLIGHTS

- Five Schiff bases from 4-methoxybenzohydrazide and hydroxybenzaldehydes.
- X-ray diffraction crystal structures of four hydrazones.
- Vibrational and electronic spectra assigned with the help of DFT calculations.

GRAPHICAL ABSTRACT

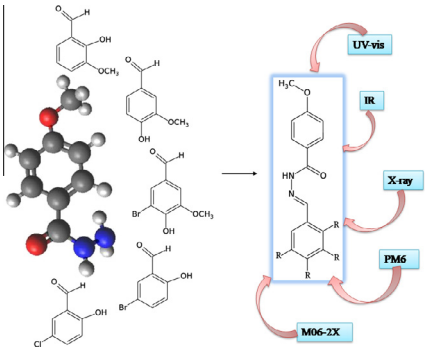

ARTICLE INFO

Article history:
Received 12 June 2014
Received in revised form 13 August 2014
Accepted 24 August 2014
Available online 6 September 2014

Keywords:
Crystal structures
DFT calculations
4-Methoxybenzohydrazide
Schiff base

ABSTRACT

Five Schiff bases obtained from condensation of 4-methoxybenzohydrazide with related aldehydes, namely *o*-vanillin, vanillin, 5-bromovanillin, 5-chlorosalicylaldehyde and 5-bromosalicylaldehyde were prepared. A detailed structural and spectroscopic study is reported. The crystal structures of four members of the family were determined and compared with one another. The hydrazones obtained from 5-chlorosalicylaldehyde and 5-bromosalicylaldehyde resulted to be isomorphic to each other. The solid-state structures are stabilized by intra-molecular O—H···N interactions in salicylaldehyde derivatives between the O—H moiety from the aldehyde and the hydrazone nitrogen atom. All crystals are further stabilized by inter-molecular H-bonds mediated by the crystallization water molecule. A comparative analysis between experimental and theoretical results is presented. The conformational space was searched and geometries were optimized both in gas phase and including solvent effects. The structure is predicted for the compound for which the crystal structure was not determined. Infrared and electronic spectra were measured and assigned with the help of data obtained from computational methods based on the Density Functional Theory.

Introduction

Schiff bases are obtained through the condensation reaction of a carbonyl compound with a species containing the NH_2 group. They have attracted considerable attention due to their potential

* Corresponding author. Tel.: +54 221 4240172.
E-mail address: agb@quimica.unlp.edu.ar (A.C. González-Baró).

http://dx.doi.org/10.1016/j.saa.2014.08.095
1386-1425/

industrial, analytical and pharmacological applications [1–6]. Moreover, Schiff bases are usually excellent chelating agents, especially when an —OH or —SH group is near the azomethine group, a structural feature that favors six member rings with the metal ion involving hydrogen bonds [7].

In particular, hydrazones obtained by condensation of hydrazides with aldehydes or ketones and their metal complexes are a research subject of continuous interest. The —C=N—N—C=O moiety present in these kind of ligands makes them optimal chelating agents. A study on the product of the reaction of the hydrazide 4-methoxybenzohydrazide (for short, MeBH; see Scheme 1) with acetone and some of its derivatives has been reported [8, and references therein]. MeBH was found to be an antileishmanial, antibacterial and antifungal agent [9 and references therein]. Also its vanadium complex was found to be a good inhibitor of urease and alpha-glucosidase [9 and references therein]. Taha and co-authors [10] reported the synthesis and antiglycation activity of 4-methoxybenzohydrazones focusing on the effect of the relative position of the OH group. However, the structures and spectroscopic behavior of the hydrazones obtained by the reaction of MeBH with aldehydes and/or ketones have not yet been described in detail.

As part of our studies on compounds of Schiff bases type, in an attempt to get more detailed information about hydrazones obtained from MeBH and with the aim of developing a new series of poly-functional ligands, we carried out a systematic study of some condensation products of MeBH with a family of hydroxy-aldehydes as summarized in Scheme 2. The aromatic aldehydes are structurally related to vanillin (4-hydroxy-3-methoxybenzaldehyde, Va), a well-known natural product, used as flavouring in food and with interesting analytical and therapeutic applications. The group includes vanillin and its isomer *o*-vanillin (2-hydroxy-3-methoxybenzaldehyde or, for short, *o*-Va) that also has well known properties [11,12], and vanillin derivative 3-bromo-4-hydroxy-5-methoxybenzaldehyde (5-bromovanillin, BrVa). Two other derivatives of salicylaldehyde are also included, namely 5-chloro-2-hydroxybenzaldehyde (5-chlorosalicylaldehyde, ClSal) and 5-bromo-2-hydroxybenzaldehyde (5-bromosalicylaldehyde, BrSal).

The present study involves a complete experimental and theoretical characterization of the five hydrazones (see Scheme 3). It is worth mentioning that the methodology employed for the syntheses and physicochemical characterization of the compounds in the present work is consistent with that used in previous studies performed in our laboratory for several different systems.

For the compounds which afforded suitable single crystals the solid state structures were determined by X-ray diffraction methods and they are disclosed here along with corresponding theoretical results. A detailed analysis of inter- and intra-molecular

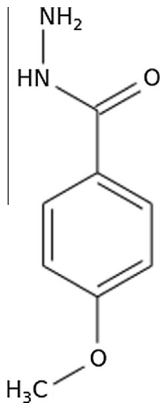

Scheme 1. Schematic representation of 4-methoxybenzohydrazide.

	R_1	R_2	R_3	R_4
o-Va	OH	OCH_3	H	H
Va	H	OCH_3	OH	H
BrVa	H	OCH_3	OH	Br
ClSal	OH	H	H	Cl
BrSal	OH	H	H	Br

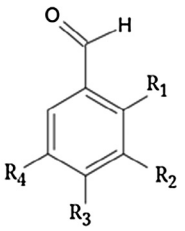

Scheme 2. Schematic representation of the aldehydes.

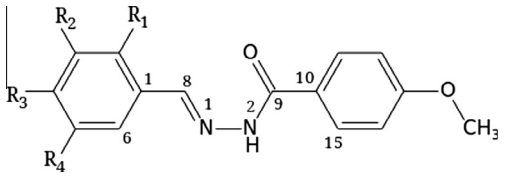

Scheme 3. Schematic representation of the obtained hydrazones; see Scheme 2 for references.

H-bonds is conducted to explain their effects on structure stabilization. Infrared and electronic absorption spectra were recorded and assigned with the help of results from computational methods based on the Density Functional Theory (DFT).

Experimental section

General procedure for the synthesis of 4-methoxybenzohydrazide Schiff bases

All chemicals were of analytic grade and used as purchased. The compounds were prepared according to an adaptation of the reported procedure for the analytical determination of the hydrazide Isoniazid with Va [13]. Ten milliliters of an ethanolic solution containing 3 mmol of the corresponding aldehyde (Sigma) was drop-wise added to a solution of 1.5 mmol of 4-methoxybenzohydrazide (Sigma) in 16 mL of ethanol (Merck), with continuous stirring and slight heating. Drops of concentrated hydrochloric acid (Merck) were added to reach a pH value of 5. Upon standing, the products were obtained and the solids were filtered and dried in a desiccator. Melting points were determined using a Bock monoscop "M" instrument.

It is worth mentioning at this point that the hydrazone obtained by the condensation reaction of MeBH with vanillin has been previously reported by other authors [10] following a different synthetic procedure. Their study was focused in the antiglycation activity of a series of compounds and it neither included spectroscopic information nor the crystal structure; furthermore, as the melting point differs from the one reported here it cannot be discarded that they could have obtained a different compound.

1.1 *N′*-(2-hydroxy-3-methoxyphenyl)methylidene-4-methoxybenzohydrazide monohydrate (**I**)
Yield: 60%
mp: 117–119 °C
Pale pink single crystals suitable for structural X-ray diffraction were grown after 24 h by slow evaporation of the solvent.

1.2 N′-(4-hydroxy-3-methoxyphenyl)methylidene-4-methoxybenzohydrazide monohydrate (**II**)
Yield: 63%
mp: 110–112 °C

Light brown single crystals suitable for X-ray diffraction were grown after ten days.

1.3 N′-(3-bromo-4-hydroxy-5-methoxyphenyl)methylidene-4-methoxybenzohydrazide (**III**)
Yield: 55%
mp: 248–250 °C
White crystalline powder unsuitable for structural X-ray study was obtained after two days.

1.4 N′-(5-chloro-2-hydroxyphenyl)methylidene-4-methoxybenzohydrazide monohydrate (**IV**)
Yield: 58%
mp: 222–224 °C
Yellow single crystals suitable for X-ray diffraction were grown after five days.

1.5 Synthesis of N′-(5-bromo-2-hydroxyphenyl)methylidene-4-methoxybenzohydrazide monohydrate (**V**)
Yield: 60%
mp: 220–222 °C
Yellow single crystals suitable for X-ray diffraction were grown after seven days.

X-ray diffraction data

The measurements were performed on an Oxford Xcalibur Gemini, Eos CCD diffractometer with graphite-monochromated Cu Kα (λ = 1.54178 Å) radiation. X-ray diffraction intensities were collected (ω scans with ϑ and κ-offsets), integrated and scaled with CrysAlisPro [14] suite of programs. The unit cell parameters were obtained by least-squares refinement (based on the angular settings for all collected reflections with intensities larger than seven times the standard deviation of measurement errors). Data were corrected empirically for absorption employing the multi-scan method implemented in CrysAlisPro. The structures were solved by direct methods with the SHELXS-97 program of the SHELX package [15] and the corresponding molecular models developed by alternated cycles of Fourier methods and full-matrix least-squares refinement on F^2 with SHELXL-97 of the same suite of programs. The same space group and nearly equal cell constants of **IV** and **V** strongly suggested the solids to be isomorphous. In fact, an initial molecular model assuming the same atom positions as in the bromide-containing crystal with the identity of the halogen atom changed from bromide to chloride lead to smooth convergence of the structural parameters for the chlorine-containing crystal during the least-squares refinement against the corresponding X-ray data set. All but the hydroxyl and water hydrogen atoms were located stereo-chemically and refined with the riding model. The methyl H-positions were optimized by treating them as rigid groups which were allowed to rotate during the refinement around the corresponding O—C bonds such as to maximize the residual electron density at their calculated positions. As a result, all CH_3 groups converged to staggered conformations. The hydroxyl H-atoms were located in a difference Fourier map and refined at their found position with isotropic displacement parameters. The water H-atoms were refined with O—H and H···H distances restrained to target values of 0.86(1) and 1.36(1) Å, respectively, and employing a common isotropic displacement parameter equal to 1.5 times the one of the water oxygen. Crystal data and structure refinement results for all four compounds are summarized in Table 1. Detailed structural parameters for all crystals are provided as supplementary material.

Spectroscopic analysis

FTIR absorption spectra (4000–400 cm^{-1}) were obtained using the KBr pellet technique in a FTIR Bruker Equinox 55 instrument with 4 cm^{-1} resolution and 60 scans. The electronic absorption spectra of the hydrazide, aldehydes and respective hydrazones were measured on ethanolic solutions (3×10^{-5} M) in the 200–800 nm spectral range. They were recorded with a Hewlett-Packard 8452-A diode array spectrometer using 10 mm quartz cells.

Computational methods

The conformational space of the compounds was explored with the aid of the semiempirical PM6 method [16]. Several starting geometries derived from selected variations in C15—C10—C9—N2, C10—C9—N2—N1, N2—N1—C8—C1 and N1—C8—C1—C6 torsion angles were optimized (see Scheme 3 for atom labeling). Geometries obtained from X-ray diffraction were also used as a starting point for the optimizations. The geometries were further re-optimized both in gas phase and including solvent effects using the hybrid meta-GGA M06-2X exchange–correlation density functional [17] with a triple-zeta 6-311G(d,p) basis set [18,19]. Solvent effects (ethanol) were included implicitly through the Conductor-like Polarizable Continuum Model [20,21]. Numerical integrations were carried out using a grid containing 96 radial points and 590 angular points around each atom. For compounds that involve Br atom (**III** and **V**), a grid with 160 radial points and 974 angular points was used. The critical points found after optimization were characterized by the sign of the eigenvalues of the Hessian matrix of the total electronic energy with respect to the nuclear coordinates. When the critical point corresponded to a minimum on the potential energy surface, the eigenvalues were converted to harmonic vibrational frequencies. Vibration frequencies were scaled by a factor of 0.982 to ease the comparison with experimental values [17]. Electronic transitions were calculated within the framework of the Time-Dependent DFT [22,23] using the PBE0 functional [24] and the triple zeta 6-311+G(d,p) basis set [18,19], with solvent effects, as was previously stated. Geometry optimizations, Hessian matrix calculation and diagonalization, and electronic transition calculations were performed with the GAMESS-US program [25]. The corresponding figures were done with Gabedit [26] and wxMacMolPlt [27].

Results and discussion

Crystallographic structural data

Fig. 1 is an ORTEP [28] drawing of **I**. Selected bond distances and angles are listed in Table 2, along with calculated data (see Conformational analysis and geometry optimization). The molecule can be described as nearly planar 3-methoxysalicylideneimino and 4-methoxybenzoylideneamido fragments (*rms* deviation of non-H atoms from the corresponding best least-squares planes are less than 0.050 Å) linked through the N—N single bond and tilted around this bond in 10.09(6)° from each other. The planarity of 3-methoxysalicylideneimino favors the formation of the observed intra-molecular O—H···N bond [d(O1···N1) = 2.696 Å, ∠(O1—H1···N1) =140.4°].

Observed bond distances and angles are in accordance with the organic chemistry's rules. In fact, C—C distances within the phenyl rings, are from 1.373(3) to 1.405(3) Å for the 3-methoxysalicylideneimino fragment and from 1.374(3) to 1.395(3) Å for the 4-methoxybenzoylideneamido one, as expected for phenyl resonant-bond structure. The short imino C8—N1 length of 1.284(3) Å contrasts with the longer amido d(C9—N2) = 1.348(3) Å value, clearly confirming the formally double and single bond character for these links. C—OH and C═O bond distances of 1.353(3) and 1.228(3) Å show expected values for the simple and double bond character of these links. The C(ph)—O—CH_3 groups show C(ph)—O distances

Table 1
Crystal data and structure refinement results for **I**, **II**, **IV** and **V** 4-methoxybenzohylhydrazones.

	I	**II**	**IV**	**V**
Empirical formula	C_{16} H_{18} N_2 O_5	C_{16} H_{18} N_2 O_5	C_{15} H_{15} Cl N_2 O_4	C_{15} H_{15} Br N_2 O_4
Formula weight	318.32	318.32	322.74	367.20
Temperature (°K)	120(2)	298(2)	293(2)	293(2)
Wavelength (Å)	1.54184	1.54184	1.54184	1.54184
Crystal system (S.G.)	Orthorhombic ($P2_12_12_1$)	Monoclinic ($P2_1/n$)	Orthorhombic ($P2_12_12_1$)	Orthorhombic ($P2_12_12_1$)
Unit cell dimensions				
a (Å)	5.0032(3)	7.9520(4)	4.4871(3)	4.4812(1)
b (Å)	12.7300(7)	21.3038(8)	6.6807(4)	6.6845(2)
c (Å)	24.097(1)	10.2390(6)	50.179(3)	51.164(2)
Volume (Å^3)	1534.8(1)	1663.11(14)	1504.2(2)	1532.61(7)
Z, calc. dens. (mg/m^3)	4, 1.378	4, 1.271	4, 1.425	4, 1.591
Abs. Coeff. (mm^{-1})	0.864	0.798	2.436	3.842
F (000)	672	672	672	744
Crystal size (mm^3)	0.32 × 0.11 × 0.08	0.27 × 0.18 × 0.09	0.19 × 0.10 × 0.05	0.490 × 0.115 × 0.044
θ-Range (°) for data collection	3.67–70.98	4.15–72.74	5.29–73.37	3.46–73.11
Index ranges	$-4 \leqslant h \leqslant 6$, $-15 \leqslant k \leqslant 11$, $-27 \leqslant l \leqslant 29$	$-8 \leqslant h \leqslant 9$, $-23 \leqslant k \leqslant 26$, $-11 \leqslant l \leqslant 12$	$-5 \leqslant h \leqslant 4$, $-8 \leqslant k \leqslant 8$, $-61 \leqslant l \leqslant 57$	$-5 \leqslant h \leqslant 3$, $-6 \leqslant k \leqslant 8$, $-62 \leqslant l \leqslant 62$
Reflections collected	4021	6749	4042	3292
Independent reflections	2488 [*R*(int) = 0.0181]	3276 [*R*(int) = 0.0205]	2588 [*R*(int) = 0.0317]	2449 [*R*(int) = 0.0164]
Observed reflections	2190	2380	0.0579	2379
Completeness	99.1% (to θ = 70.98°)	98.9% (to θ = 72.74°)	98.7% (to θ = 73.37°)	98.3% (to θ = 73.11°)
Max. and min. transmission	0.9341 and 0.7677	0.9302 and 0.8129	0.8962 and 0.6547	0.8492 and 0.2547
Refinement method	Full-matrix least-squares on F^2	Full-matrix least-squares on F^2	Full-matrix least-squares on F^2	Full-matrix least-squares on F^2
Data/restraints/parameters	2488/3/220	3276/0/222	2588/3/210	2449/3/210
Goodness-of-fit on F^2	1.092	1.017	1.107	1.214
Final *R* indices[a] [$I > 2\sigma(I)$]	*R*1 = 0.0394, *wR*2 = 0.0954	*R*1 = 0.0440, *wR*2 = 0.1146	*R*1 = 0.0579, *wR*2 = 0.1472	*R*1 = 0.0680, *wR*2 = 0.1781
R indices (all data)	*R*1 = 0.0457, *wR*2 = 0.1021	*R*1 = 0.0623, *wR*2 = 0.1312	*R*1 = 0.0686, *wR*2 = 0.1556	*R*1 = 0.0699, *wR*2 = 0.1789
Absolute structure parameter	−0.1(3)		0.01(4)	0.00(7)
Largest diff. peak and hole (e Å^{-3})	0.129 and −0.189	0.140 and −0.160	0.402 and −0.282	0.651 and −0.688

[a] $R_1 = \Sigma||F_o| - |F_c||/\Sigma|F_o|$, $wR_2 = [\Sigma w(|F_o|^2 - |F_c|^2)^2/\Sigma w(|F_o|^2)^2]^{1/2}$.

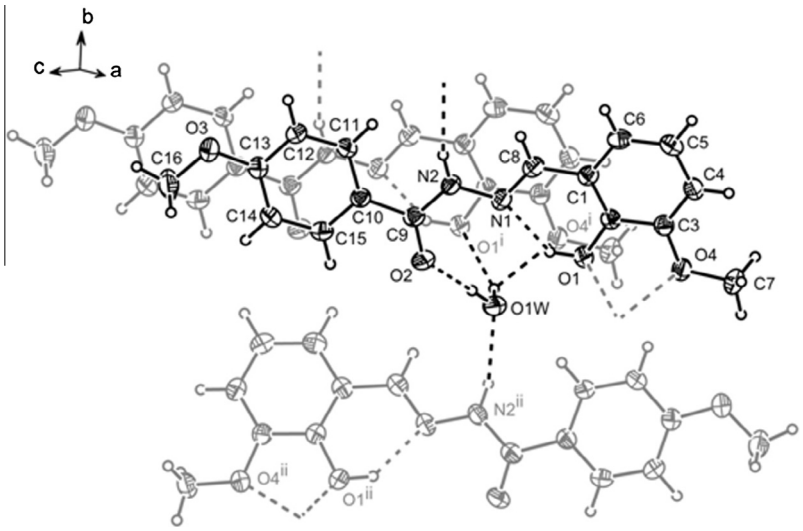

Fig. 1. View of **I** crystal, showing the labeling of the non-H atoms and their displacement ellipsoids at the 30% probability level. H-bonds are indicated by dashed lines. Symmetry operations: (i) $-1 + x, y, z$; (ii) $1 - x, -1/2 + y, 1/2 - z$.

[1.363(3) and 1.371(3) Å] shorter than the O—CH_3 ones [1.415(3) and 1.426(3) Å].

Fig. 2 shows a plot of **II**. Selected bond distances and angles are in Table 2. Molecule **II** is an isomer of **I**, since the respective aldehydes differ in the location of the hydroxyl group in the phenyl ring. Structurally, **I** and **II** differ only in a 180° rotation of the methoxy group around the C—OCH_3 bond of the methoxy-hydroxysalicylideneimino fragment. This on one hand removes the intramolecular OH···N bond present in **I** and on the other it affords the formation of an strong O—H···Ow bond with the crystallization water molecule [d(O1···O1w) = 2.585 Å, ∠(O1—H···O1w) = 175.6°] and a HO···H—N bond with a neighboring **II** molecule [d(O1···N2′) = 3.048 Å, ∠(O1···H—N2′) = 159.9°].

The degree of isomorphism between the chloride- and bromide-containing molecules in the **IV** and **V** solids is very high. In fact, the *rms* separation between all homologous non-H atoms but the halide atoms in the best least-squares structural fitting, calculated by the Kabsh's procedure [29], is 0.026 Å. C(ph)—X bond lengths

Table 2
Comparison of selected experimental and calculated geometrical parameters. Calculated values were obtained at the M06-2X/6-311G(d,p) level of theory. X = H for **I** and **II**, X = Br for **III** and **V**, and X = Cl for **IV**. See schemes and Figs. 1–3 for the atom labeling scheme.

	I		**II**		**III**	**IV**		**V**	
	Exp.	Calc.	Exp.	Calc.	Calc.	Exp.	Calc.	Exp.	Calc.
Bond lengths (Å)									
N1···HO1	2.292	1.843	–	–	–	1.902	1.755	1.816	1.851
O1w···HO1	2.735	–	1.719	–	–	2.538	–	2.603	–
C13—O3	1.364	1.351	1.367	1.352	1.352	1.364	1.350	1.359	1.350
C5—X	0.950	1.082	0.930	1.085	1. 903	1.744	1.751	1.895	1.899
Bond angles (°)									
N1—H—O1	143.7	142.0	–	–	–	141.7	143.4	146.3	141.6
C13—O3—C16	118.0	117.8	124.9	117.8	117.9	117.1	118.2	117.0	117.9
H—O1—C4	–	–	113.7	108.9	109.2	–	–	–	–
Torsion angles (°)									
C15—C10—C9—N2	−175.8	−30.2	164.9	156.7	157.4	−167.5	−151.9	−165.7	153.2
C10—C9—N2—N1	−179.2	−19.2	176.6	179.0	−170.8	177.7	−178.3	177.5	−20.2
N2—N1—C8—C1	−179.5	−179.0	−179.8	179.4	−179.7	179.6	−179.6	178.6	−179.2
N1—C8—C1—C6	−176.8	−179.5	176.6	−179.4	178.7	−179.1	−179.4	−179.4	−180.0
C3—C2—O1—H	173.0	174.5	–	–	–	−176.9	179.4	178.4	179.7
C14—C13—O3—C16	1.6	1.0	3.1	0.4	−179.8	−178.2	179.8	−178.1	0.9

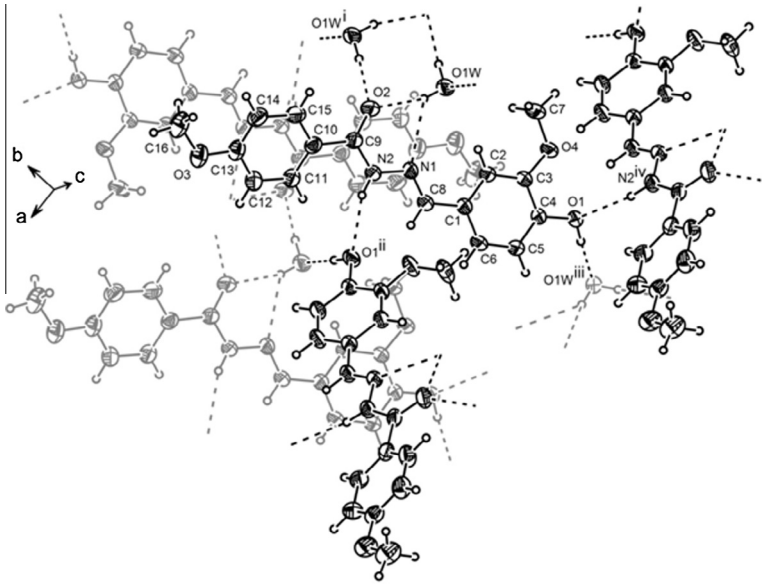

Fig. 2. View of **II**. Symmetry operations: (i) 1 − *x*, 1 − *y*, −*z*; (ii) 0.5 + *x*, 0.5 − *y*, −0.5 + *z*; (iii) 0.5 + *x*, 0.5 − *y*, 0.5 + *z*; (iv) −0.5 + *x*, 0.5 − *y*, 0.5 + *z*.

are 1.744(4) Å for X = Cl and 1.895(10) Å for X = Br. Fig. 3 shows a plot of the bromide compound.

Furthermore, **IV** and **V** molecules are closely related to **I** molecule, only differing in a 180° rotation of the methoxy group around the C—OCH_3 bond of the common 4-methoxybenzoylideneamido fragment, besides the different substituents in the aldehyde rings. In **IV** and **V** isomorphous compounds, the 4-methoxybenzoylideneamido and (5-X-2-hydroxyphenyl, with X = Cl in **IV** and Br in **V**) methylidene fragments are tilted around the linking N—N bond in 17.9(1)° for **IV** and 17.7(3)° for **V**. The crystals are further stabilized by inter-molecular H-bonds mediated by a water molecule. In **I** the water bridges three neighboring symmetry-related molecules, two of them acting as acceptors in Ow—H···O interactions involving the carbonyl oxygen of one molecule and both the hydroxyl and methoxy oxygen atoms of a second molecule. The third molecule acts as H-donor in an N—H···Ow interaction (see Fig. 1). **II**, **IV** and **V** crystals exhibit similar H-bonding structures (see Figs. 2 and 3). Detailed H-bond distances and angles for all four crystals are provided as supplementary material. Furthermore, **I**, **IV** and **V** crystals present intra-molecular H1···N1 bonds, being 1.942 for **I**, 1.902 Å for **IV** and 1.816 for **V** (see Supplementary Material for detailed structural parameters), suggesting that the intra-molecular H-bond is affected by the volume of the substituent in the 5-position of the aldehyde fragment.

Conformational analysis and geometry optimization

As it was previously mentioned, calculations were performed using DFT tools, both in the gas phase and including solvent effects, at the M06-2X/6-311G(d,p) level of theory. Geometries optimized from X-ray structures with solvent effects were found to be the lowest-energy structures. Selected calculated structural parameters are listed in Table 2, together with the experimental counterparts, which were already discussed in the previous sub-section. Calculated parameters for compound **III** are included for comparison with other compounds, as no experimental information exists yet.

It is found in the table that calculated N1···HO1 hydrogen bond distances are underestimated for **I** and **IV**. It is argued that the water molecule in the crystals interacts with the HO1 group form-

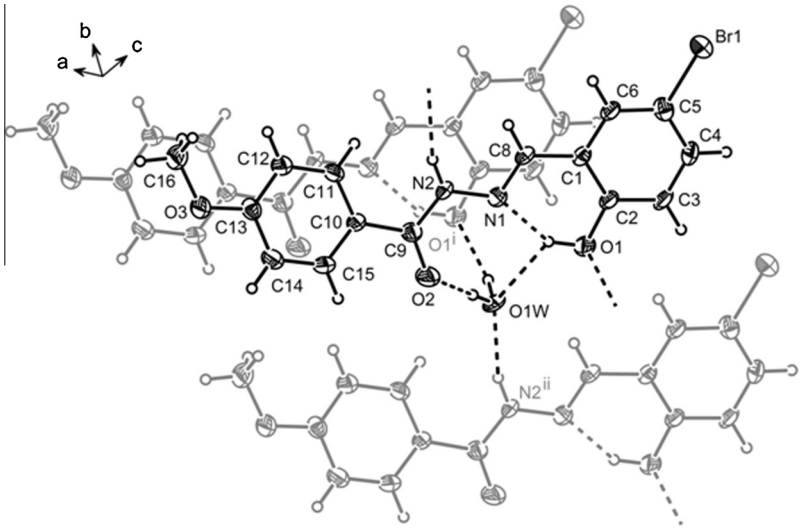

Fig. 3. View of the bromide-containing crystal of the isomorphous **IV** and **V** compounds. Symmetry operations: (i) $1 + x, y, z$; (ii) $x, -1 + y, z$.

ing a O1w···HO1 bond, thus diminishing the strength of the former N1···HO1 bond. That decrease in the strength of the hydrogen bond is not evidenced by the calculations as the water molecule is not considered. It can also be seen in the table that the C5—X distance is well reproduced both when X is H and when X is Cl or Br. Also, it is observed that the C13—O3 bond distance remains almost unaltered along the series. This is an expected finding as this part of the hydrazones is not involved in any inter- or intra-molecular hydrogen bonds. Bond angles are in general well described by the present level of theory, with errors not greater than 5°. Calculated torsion angles are in good agreement with experimental data as can be deduced from Table 2. The exceptions are the C15—C10—C9—N2 and C10—C9—N2—N1 torsion angles, for which important discrepancies exist in **I** and **V**, and the C14—C13—O3—C16 one, for which an appreciable departure from the experimental value is observed in **V**. These discrepancies could be attributed to lattice effects that stabilize geometries that are not found when calculations including implicit solvent effects are carried out on isolated molecules. On the other hand, calculated structural parameters for compound **III** are in good agreement with those found experimentally for the other Schiff bases, suggesting that the present level of theory could be helpful to elucidate the structure of novel Schiff bases.

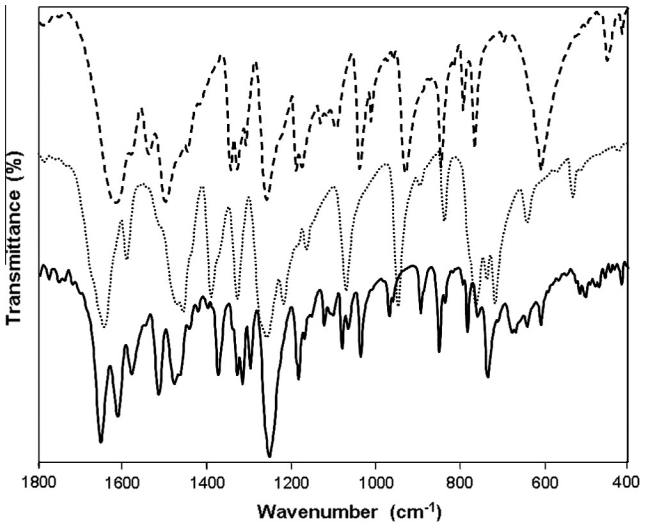

Fig. 4. Experimental IR spectrum of *o*-Va (···), MeBH (——) and **I** (—), in the 1800–400 cm^{-1} spectral range.

Vibrational spectroscopy

The infrared spectra of the solids were recorded and their vibrational properties were examined with the help of data obtained from calculations based on the Density Functional Theory. The spectra of MeBH, the aldehydes and the Schiff bases, were registered in the 400–4000 nm spectral range. Fig. 4 shows, with illustrative purpose, the experimental infrared spectrum of compound **I**, together with *o*-Va and MeBH spectra in the more relevant spectral range, namely 1800–400 cm^{-1}. IR spectra of compounds **II** to **V** are provided as supplementary material.

The experimental and calculated values along with the proposed assignment of relevant bands, characteristic of hydrazone formation or sensitive to the nature of the substituents, are available as supplementary material (Tables S6a–e) and compared with the data of MeBH and the respective aldehyde IR spectra. The assignments of the spectra were done with the aid of calculated normal mode frequencies of the gas phase structures and taking into account the predominant modes at each frequency. The assignments are in agreement with data reported previously [12,30]. The bands at higher frequencies, between 3570 and 3410 cm^{-1}, are assigned to crystallization water molecules that were not considered in the calculations. Calculations show a strong coupling between several modes.

Table 3 shows a selected set of experimental IR bands of compounds **I**–**V** compared with those of MeBH and the respective aldehydes.

The IR spectra of the compounds show weak bands corresponding to OH stretching modes between 3006 cm^{-1} and 3085 cm^{-1} and to the C8H stretching vibrations between 2839 cm^{-1} and 2975 cm^{-1} in the Schiff bases (for atom numbering see Scheme 3 and Figs. 1–3). Calculated values of the O—H stretching frequencies are higher than the experimental ones, as H-bond interactions, present in the hydrazones and in the aldehydes, are neglected in the calculations. This last mode remains observable at almost the same frequency after condensation in **III**, **IV** and **V** hydrazones. It is observed that the band assigned to rings ν CH modes appear between 3102 and 3080 cm^{-1} in **I**; 3054 and 2967 cm^{-1} in **II**; 3180 and 3117 cm^{-1} in **III**; 3100 and 2972 in **IV**; and 3173 and

Table 3
Selected experimental bands of the **I–V** Shift bases IR spectra. Values for MeBH and the respective aldehydes are included for comparison. Complete assignments of relevant bands and calculated frequencies are available as Supplementary Material (Tables S6a–e).

Assignment	MeBH	*o*-Va	**I**	Va	**II**	BrVa	**III**	ClSal	**IV**	BrSal	**V**
ν OH		3014 w	3006 vw	3018 w	3085 w	3073 w	3072 vw	3047 vw	3050 wb	3042 vw	3047 wb
ν C═O	1614 vs, b	1645 vs	1650 s	1665 vs	1640 s	1676 vs	1641 s	1663 vs	1647 s	1672 vs	1647 s
ν C═N			1608 s, b		1598 s		1606 s		1608 s		1610 s
δ OH		1388 s	1371 m	1430 s	1415 m	1426 s	1420 m	1378 s	1358 m	1373 m	1355 m
ν Ar—OH		1327 s	1327 m	1300 m	1287 s	1354 s	1295 s	1304 m	1291 m	1305 mw	1291 s
ν N—N	1188 m		1181 w		1180 m		1185 s		1193 m		1193 m
γ OH		838 m	836 m	858 s	841 s	854 s	867 m	831 s	824 m	892 m	878 m
γ NH	453 w		472 vw		473 w		467 vw		472 w		473 w

2970 in **V**. Additionally, the bands are blue-shifted in comparison with the CH stretching mode of MeBH. Despite the fact that calculated values are higher than experimental ones, they allow discerning between modes of the aldehyde ring from the ones of MeBH ring in the hydrazone. A strong band is observed at 1650 cm^{-1} for **I**, 1640 cm^{-1} for **II**, 1641 cm^{-1} for **III**, and 1647 cm^{-1} for **IV** and **V,** characteristic of the C═O stretching. It is seen that the C═O stretching mode is blue-shifted in comparison with this mode in the sole hydrazide (observed at 1614 cm^{-1}). The C═O band in the MeBH spectrum is broader than in the hydrazones, as it is coupled with the NH_2 bending mode, absent in the Schiff bases. An additional strong band is observed in the 1598–1610 cm^{-1} range, characteristic of the C═N stretching mode, which appears due to the formation of the hydrazone. This mode seems to be insensitive to the nature and position of the substituent in the aldehyde ring. It is observed that calculated values are overestimated for OH, C═O and C═N stretching modes, possibly due to the lack of restrictions in the gas phase that are present in the solid (see Supplementary Material). It must be noted that the H atom bonded to O1, the O2 atom of C═O moiety and the N1 atom of C═N group are involved in H-bonds in all crystals (see Figs. 1–3). As expected, the bands related to the NH_2 group of MeBH (at 3323, 3204 and 1307 cm^{-1}) are absent in the hydrazones spectra. After a thorough analysis of the experimental results and with the help of calculated data, we could identify ring stretching modes and Ar—OH or Ar—OCH_3 groups present in the hydrazones. Moreover, it was possible to discriminate between modes related either to the aldehyde or to the MeBH fragments of the molecules (see Tables S6a–e). Bands assigned to ring stretching modes appear at expected spectral range and have similar behavior for the five Schiff bases. Regarding the MeBH ring stretching (1535 cm^{-1}), the band frequencies are blue-shifted, and with respect to the aldehydes, they are red-shifted, except for **III**, in which the band remains at the same frequency (1502 cm^{-1}). Calculated frequencies are about 80 cm^{-1} higher than experimental values. Each experimental ring stretching band in the hydrazones is described by two calculated frequencies, one of them for the MeBH fragment mode and the other for the aldehyde one. The NH bending mode does not show a definite behavior along the series; nonetheless, it is noticed that it is coupled with different modes in the hydrazones. The OH bending in the aldehydes spectra appears between 1373 cm^{-1} and 1388 cm^{-1} in salycilaldehyde derivatives and around 1430 cm^{-1} in vanillin derivatives. It is generally red-shifted upon condensation and appears coupled with other hydrazone modes.

Several characteristic modes of MeBH are conserved after condensation. In particular, the strong bands at 1258 cm^{-1} assigned to C—C(O)—N stretching and at 1037 cm^{-1} assigned to ring deformation in the hydrazide are located in the 1252–1262 cm^{-1} and 1025–1049 cm^{-1} ranges, respectively, in the hydrazones spectra. Moreover, CH out-of-plane bending, appearing at 845 cm^{-1} in MeBH, shows only slight shifts in compounds **I** to **V.**

The band assigned to ν N—N in MeBH is conserved in the Schiff bases and appears between 1180 and 1193 cm^{-1}. This mode is coupled with others in de hydrazones. Vibrational modes corresponding to OH and NH out-of-plane deformations (γ) are also present in the Schiff bases. These modes do not show a regular trend in their frequencies, but it is observed that the calculated values in the vanillin derivatives are notoriously lower than in the salycilaldehyde derivatives. In addition, this mode is coupled with other modes only in salycilaldehyde derivatives. C═O out-of-plane deformation is also conserved in the hydrazones. The respective bands are less intense than that of MeBH. Bending modes of the CO—NH—H moiety (characteristic of the hydrazones) are found in the 618–715 cm^{-1} range for salycilaldehyde derivatives, and at 422 cm^{-1} for **II**, and 449 cm^{-1} for **III**. Furthermore, the C—Cl stretching mode of **V** is found to be coupled with the mentioned bending mode, giving rise to a band located at 715 cm^{-1}. The C—Br stretching mode is observed at 524 cm^{-1} in **III** and at 561 cm^{-1} in **V**. The difference in frequencies can be attributed to bond weakening of **III** due to the presence of the methoxy substituent in the ring.

Electronic spectroscopy

The electronic absorption spectra of MeBH, the aldehydes and the Schiff bases, were registered in the 200–800 nm spectral range. Experimental electronic spectrum of compound **I** is depicted in Fig. 5, together with *o*-Va and MeBH spectra, as illustrative example.

Analogous sets of MeBH, aldehyde and hydrazone comparative spectra for compounds **II** to **V** are included as supplementary material. In Table 3 experimental absorption bands and calculated electronic transitions are listed, together with the proposed assignments. Figures of the molecular orbitals involved in the electronic

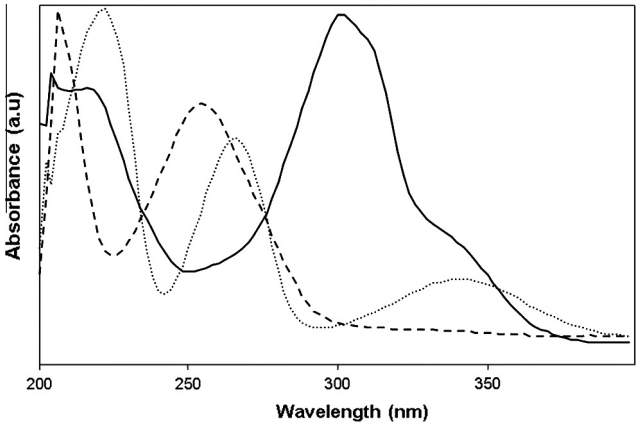

Fig. 5. Experimental electronic spectrum of 3×10^{-5} M ethanolic solutions of *o*-Va (···), MeBH (——) and **I** (—).

transitions are also available as supplementary material. The assignments were accomplished on the basis of calculated electronic transitions. It can be seen from Table 4 that the calculated transitions describe very well the experimental electronic spectra.

General description of MOs

From calculations it can be seen that many-body effects are far from negligible. Most of the transitions are described by two or more one-electron excitations, involving several MO's. It can be appreciated from Table 4 that the same set of MO's is involved in the calculated transitions of compounds **I** to **V**, that is from HOMO−5 to HOMO and from LUMO to LUMO+3. The assignment of experimental bands, however, is performed using different combinations of those MO's for every compound. A general description of the character of the MO's is provided in the following paragraphs and a more detailed discussion of the features of the electronic spectrum of compounds **I** to **V** is given in the next sub-sections.

The HOMO is π in character in the aldehyde ring, with minor non-bonding contributions from oxygen atoms of the OH, C═O and O—CH_3 groups in the aldehyde fragment, when it corresponds. For Schiff bases **II**–**V**, the HOMO is also π in character in the C═N moiety and, for **IV** and **V**, it is non-bonding in the halogen atom. For hydrazones **II**–**V**, the HOMO−1 is π in character in the MeBH ring and non-bonding in the O atom of the O—CH_3 group of MeBH. For **I**, on the other hand, the HOMO−1 is π in character in both rings and in the C═N moiety, with minor contributions from non-bonding interactions in the nitrogen atom of the —NH group and oxygen atoms of the OCH_3 and C═O groups. The HOMO−2 is very similar to HOMO for compounds **II**–**V**, including non-bonding contribution from halogen atoms in **III**–**V**. In **I**, the HOMO−2 is mostly π in character in the MeBH ring and in the C═N moiety. The HOMO−3 is π in character in the MeBH ring with minor non-bonding contributions from oxygen atoms of the C═O group. In compound **III**, the HOMO−4 is π in character in the C═N moiety with non-bonding contributions from the nitrogen atom of the —NH group and the oxygen atoms of all groups, except for the OCH_3 group in the MeBH fragment. The HOMO−5 is π in character in the aldehyde ring in salycilaldehyde derivatives **I**, **IV** and **V**, and it is non-bonding in the oxygen atoms in vanillin derivatives **II** and **III**.

The LUMO is π anti-bonding in the Ar—C bond, carbon atoms of rings, nitrogen atom of C═N group and at the C═O group. The LUMO+1 is π* in character in the MeBH ring and is also localized at the nitrogen atoms and at the oxygen atom of the C═O moiety. The LUMO+2 is π anti-bonding in the carbon atoms of MeBH in compound **I** and is π* in character in the aldehyde ring of halogenated Schiff bases **III** and **IV**. Finally, the LUMO+3 is π anti-bonding in the carbon atoms of *o*-Va in **I** and is π* in character in the aldehyde ring for compounds **II**–**V**.

Table 4
Electronic spectra of 3×10^{-5} M ethanolic solutions of the compounds. Calculated electronic transitions are also shown. Only those calculated electronic transitions relevant for the assignments are listed. Wavelength absorption maxima are given in nm. Oscillator strengths of calculated transitions, shown in parenthesis, are in atomic units.

Exp.	Calc.	Assignment
I		
204	207 (0.1838)	HOMO−3 → LUMO+1 (60%)
		HOMO−2 → LUMO+2 (14%)
218	223 (0.2297)	HOMO → LUMO+3 (42%)
		HOMO−5 → LUMO (17%)
302	276 (0.1914)	HOMO−2 → LUMO (93%)
312	297 (0.5753)	HOMO−1 → LUMO (96%)
333	326 (0.0753)	HOMO → LUMO (96%)
II		
210	219 (0.1541)	HOMO−2 → LUMO+1 (56%)
236	236 (0.2498)	HOMO−1 → LUMO+1 (37%)
		HOMO−5 → LUMO (24%)
257	244 (0.4469)	HOMO → LUMO+3 (36%)
		HOMO−2 → LUMO (34%)
302	276 (0.1114)	HOMO−1 → LUMO (78%)
327	317 (0.6379)	HOMO → LUMO (97%)
III		
206	212 (0.1603)	HOMO−2 → LUMO+2 (70%)
216	232 (0.1275)	HOMO−5 → LUMO (26%)
		HOMO−4 → LUMO (27%)
		HOMO−3 → LUMO (21%)
307	245 (0.4855)	HOMO → LUMO+2 (40%)
		HOMO−1 → LUMO+1 (19%)
		HOMO−2 → LUMO (19%)
326	315 (0.6280)	HOMO → LUMO (97%)
IV		
209	209 (0.1540)	HOMO−5 → LUMO (56%)
214	232 (0.1007)	HOMO−1 → LUMO+1 (57%)
		HOMO → LUMO+2 (21%)
241	233 (0.1393)	HOMO−3 → LUMO (37%)
		HOMO → LUMO+2 (36%)
279	239 (0.2000)	HOMO → LUMO+3 (53%)
		HOMO−1 → LUMO+1 (20%)
290	270 (0.1880)	HOMO−2 → LUMO (76%)
302	290 (0.4305)	HOMO−1 → LUMO (87%)
339	326 (0.6067)	HOMO → LUMO (97%)
V		
210	206 (0.0646)	HOMO−2 → LUMO+3 (36%)
246	219 (0.0769)	HOMO−5 → LUMO+1 (56%)
279	233 (0.1971)	HOMO−3 → LUMO (36%)
280	241 (0.2044)	HOMO → LUMO+3 (53%)
292	270 (0.1479)	HOMO−2 → LUMO (74%)
302	292 (0.5031)	HOMO−1 → LUMO (88%)
339	329 (0.5862)	HOMO → LUMO (97%)

*Electronic spectrum of **I***

According to the above analysis and the data from Table 4, the band at 204 nm can be mainly assigned to a transition from the *o*-Va ring to the MeBH ring and Ar—C bonds. The band at 218 nm is assigned to a transition involving the *o*-Va moiety, with contributions from the —NH, C═O and C═N groups. The band observed at 302 nm is assigned to the overlapping of a transition involving the MeBH moiety with a transition from the *o*-Va ring to the MeBH one, involving the C═O and —NH groups. The bands at 312 nm and 333 nm are assigned to transitions from the rings to Ar—C bonds and to the C═O and C═N groups.

*Electronic spectrum of **II***

On the basis of the description of the MO's given above and the data from Table 4, the band located at 210 nm can be assigned mainly to a π → π* transition from the Va ring to the MeBH ring with some contributions of the C═N group. The observed band at 236 nm is assigned to a π → π* transition from both MeBH and Va rings to the Va ring with minor contributions from the nitrogen atom of the —NH moiety and the oxygen atoms of all groups. The band at 257 nm is assigned mainly to a π → π* from the Va ring to the MeBH ring. The band at 290 nm is also assigned to π → π* transition from the Va ring to both the Va and MeBH rings. The bands observed at 302 nm and 327 nm are assigned to a transition from the Va ring to the C—C, C═O and C═N groups.

*Electronic spectrum of **III***

On account of the provided descriptions of the MOs and the electronic spectra described in Table 4, the band at 206 nm can be assigned to a π → π* transition from the BrVa ring and the C═N bond to the MeBH ring. The band at 212 nm is assigned to a π → π* transition involving the BrVa ring. The band at 216 nm is assigned to a π → π* transition from the BrVa ring to the MeBH one. The band at 236 nm is attributed mainly to a π → π* transition involving both Va and MeBH rings. The band at 240 nm is assigned

to a $\pi \rightarrow \pi^*$ transition involving both BrVa and MeBH rings. The bands at 260 nm and 338 nm are assigned mainly to $\pi \rightarrow \pi^*$ transitions from the BrVa ring to C—C bonds. The band at 294 nm is assigned to a $\pi \rightarrow \pi^*$ transition from both Va and MeBH rings to the C—C bonds, with contributions from the nitrogen atom of the C═N group and the oxygen atoms of the C═O and —OH groups.

Electronic spectrum of ***IV***

Based on the given description of the MOs and the data listed in Table 4, the band at 209 nm is assigned to a $\pi \rightarrow \pi^*$ transition in the ClSal ring, with minor contributions from the C═O and —NH groups. The band at 214 nm is due to a $\pi \rightarrow \pi^*$ transition from the ClSal ring to the MeBH ring with contributions from the C═O and —NH groups. The band at 222 nm is assigned to a $\pi \rightarrow \pi^*$ transition from the ClSal ring to the MeBH ring and other transitions from the MeBH ring to the ClSal ring and to the C—C bonds. The band at 240 nm is assigned to transitions involving the ClSal ring and the C═N, —NH and —OH groups. The bands at 280 nm and at 336 nm are attributed to a $\pi \rightarrow \pi^*$ transition involving the ClSal ring and the C═N, C═O and —OH groups. The band at 290 nm is assigned to a $\pi \rightarrow \pi^*$ transition from the ClSal ring to the MeBH one with some minor contributions involving oxygen atoms.

Electronic spectrum of ***V***

Based on the description of the MOs given above and the data from Table 4, the band at 210 nm is due to a transition involving the BrSal ring with minor contributions from oxygen atoms and nitrogen atoms. The band at 246 nm is assigned to a $\pi \rightarrow \pi^*$ transition from the BrSal ring to the MeBH ring, with minor contributions from the bromine atom, the nitrogen atom in the —NH moiety and the oxygen atom in the C═O group. The bands at 279 nm and 302 nm are assigned to a $\pi \rightarrow \pi^*$ transition from the MeBH ring to the BrSal ring, with minor contributions from the C═O group. The band at 280 nm is due to a $\pi \rightarrow \pi^*$ transition involving the BrSal ring. The bands at 292 nm and 339 nm are assigned to a $\pi \rightarrow \pi^*$ transition from the BrSal ring to the MeBH ring, with minor contributions from the bromine atom, the nitrogen atom in the —NH moiety and the oxygen atoms in the OH and C═O groups.

Conclusions

Five hydrazone Schiff bases are obtained as products of the condensation reactions between 4-methoxybenzohydrazide and the respective hydroxybenzaldehydes. Four of the compounds were obtained as single crystals suitable for X-ray diffraction studies and their solid-state structures are reported here. All but one resulted to be orthorhombic and the two hydrazones obtained from halogenated derivatives of salycilaldehyde turned out to be isomorphic to each other. The solids are further stabilized by intra- and inter-molecular H-bonds. The geometric features predicted by calculations agree very well with the structural parameters obtained from crystallographic data. In particular, for the polycrystalline hydrazone obtained from Br-vanillin, calculated geometrical data was valuable as it agrees very well with that obtained for the other members of the family. IR absorption bands denoting the formation of the Schiff bases were identified and assigned. Furthermore, the influence of the nature and relative position of the substituents was analyzed and discussed. Calculated harmonic frequencies assisted the complete assignment of the experimental vibration spectra. Moreover, a strong coupling between several modes at each calculated frequency is described by theoretical results. As expected, the electronic absorption spectra of the compounds in solution are similar. They were assigned with the help of calculated data. According to the calculations, most transitions can be described by two or more one-electron excitations involving several molecular orbitals. The calculated excitation energies are consistent with the observed electronic absorption bands.

Acknowledgments

This work was supported by CONICET (CCT-La Plata), UNLP and ANPCyT, Argentina. V.F.C. is a Post-doctoral Fellow of CONICET. G.A.E., O.E.P., R.P.D. and A.C.G.B. are members of the Research Career of CONICET.

Appendix A. Supplementary material

Supplementary data associated with this article can be found, in the online version, at http://dx.doi.org/10.1016/j.saa.2014.08.095.

References

[1] M. Behpour, S.M. Ghoreishi, N. Mohammadi, N. Soltani, M. Salvati-Niasari, Corros. Sci. 52 (2010) 4046–4057.
[2] H. Temel, S. Pasa, Y.S. Ocak, I. Yilmaz, S. Demir, I. Ozdemir, Synth. Met. 161 (2012) 2765–2775.
[3] A.H. Kianfar, M. Paliz, M. Roushani, M. Shampisur, Spectrochim. Acta A 82 (2011) 44–48.
[4] A.A. Khandar, C. Cardin, S.A. Hosseini-Yazdi, J. McGrady, M. Abedi, S.A. Zarei, Y. Gan, Inorg. Chim. Acta 363 (2010) 4080–4087.
[5] I. Yilmaz, H. Temel, H. Alp, Polyhedron 27 (2008) 125–132.
[6] A.A. Nejo, G.A. Kolawole, A.O. Nejo, J. Coord. Chem. 63 (2010) 4398–4410.
[7] P.A. Vigato, S. Tamburini, Coord. Chem. Rev. 248 (2004) 1717–2128 (and references therein).
[8] S. Pal, J. Pushparaju, N.R. Sangeetha, S. Pal, Trans. Met. Chem. 25 (2000) 529–533.
[9] U. Ashiq, R.A. Jamal, M.N. Tahir, S. Yousuf, I.U. Khan, Acta Cryst. E 65 (2009) o1551.
[10] M. Taha, H. Naz, S. Rasheed, N.H. Ismail, A.A. Rahman, S. Yousuf, M.I. Choudhary, Molecules 19 (2014) 1286–1301.
[11] A. Blagus, D. Cinčić, T. Friščić, B. Kaitner, V. Stilinovic, Maced. J Chem. Eng. 29 (2010) 117–138.
[12] A.C. González-Baró, R. Pis-Diez, B.S. Parajón-Costa, N.A. Rey, J. Mol. Struct. 1007 (2012) 95–101.
[13] E.F. Oga, Int. J. Pharm. Pharm. Sci. 2 (2010) 55–58.
[14] CrysAlisPro, 1.171.33.48 ed., Oxford Diffraction Ltd.: release 15–09-2009 CrysAlis171.NET.
[15] G.M. Sheldrick, Acta Crystallogr. A A64 (2008) 112–122.
[16] J.J.P. Stewart, J. Mol. Model. 13 (2007) 1173–1213. MOPAC2012; James J.P Stewart, Stewart Computational Chemistry, Colorado Springs, CO, USA, 2012. http://OpenMOPAC.net.
[17] Y. Zhao, D.G. Truhlar, Theor. Chem. Acc. 120 (2008) 215–241.
[18] R. Krishnan, J.S. Binkley, R. Seeger, J.A. Pople, J. Chem. Phys. 72 (1980) 650–654.
[19] T. Clark, J. Chandrasekhar, P.V.R. Schleyer, J. Comput. Chem. 4 (1983) 294–301.
[20] V. Barone, M. Cossi, J. Phys. Chem. A 102 (1998) 1995–2001.
[21] M. Cossi, N. Rega, G. Scalmani, V. Barone, J. Comput. Chem. 24 (2003) 669–681.
[22] A. Dreuw, M. Head-Gordon, Chem. Rev. 105 (2005) 4009–4037.
[23] P. Elliott, F. Furche, K. Burke, in: K.B. Lipkowitz, D.B. Boyd (Eds.), Reviews in Computational Chemistry, vol. 26, VCH, New York, 2009, pp. 91–165.
[24] C. Adamo, V.J. Barone, Chem. Phys. 110 (1999) 6158–6170.
[25] M.W. Schmidt, K.K. Baldridge, J.A. Boatz, S.T. Elbert, M.S. Gordon, J.H. Jensen, S. Koseki, N. Matsunaga, K.A. Nguyen, S.J. Su, T.L. Windus, M. Dupuis, J.A. Montgomery, J. Comput. Chem. 14 (1993) 1347–1363. GAMESS-US version 1 October 2010 (R1).
[26] A.R.J. Allouche, Comput. Chem. 32 (2011) 174–182.
[27] B.M. Bode, M.S. Gordon, J. Mol. Graph. Model. 16 (1998) 133–138.
[28] C.K. Johnson, ORTEP-II, Report ORNL-5318; Oak Ridge National Laboratory, Oak Ridge, TN, 1976.
[29] W. Kabsch, Acta Cryst. A 32 (1976) 922–923.
[30] E.A. Velcheva, B.A. Stamboliyska, P.J. Boyadjieva, J. Mol. Struct. 963 (2010) 57–62.